Supplementary Information

Spectroscopic Observation and Ultrafast Coherent Vibrational Dynamics of the Aqueous Phenylalanine Radical

Muhammad Shafiq Bin Mohd Yusof,[1] Jing Xuan Siow,[1] Ningchen Yang,[1] Wei Xin Chan,[1] Zhi-Heng Loh[1,*]

[1]Division of Chemistry and Biological Chemistry, School of Physical and Mathematical Sciences, Nanyang Technological University, 21 Nanyang Link, Singapore 637371, Singapore

* Corresponding author. E-mail: zhiheng@ntu.edu.sg

Section S1: Photon-order Measurements for the Strong-field Photodetachment of the Phenylalaninate Anion in Aqueous Solution

A power-dependence measurement is performed to determine the photon order of the strong-field photodetachment process of the phenylalaninate anion in aqueous solution. For an N-photon photodetachment process, the differential absorption signal, ΔA, scales with intensity of the ionizing pump, I, as $\Delta A \propto I^N$. The photon-order measurements are performed by using a UV probe, which measures the absorption of the radical at a pump-probe time delay of 1 ps and at a probe wavelength of ~308 nm, corresponding to the maximum absorption of the Phe• radical. Hence, the absorption signal observed is proportional to the photodetachment yield.

To determine the photon order of the photodetachment process accurately, one must consider that electrons can originate from both the phenylalaninate and hydroxide anions during the photodetachment of the alkaline phenylalaninate solution. To account for the contribution from the photodetachment of hydroxide anions, we record the ΔA spectrum against the pump intensity for both the aqueous phenylalaninate and aqueous sodium hydroxide solutions under similar experimental conditions. The difference ΔA spectrum, i.e., the $\Delta\Delta A$ spectrum, is then obtained, which in principle corresponds to solely the ΔA signal from the photodetachment of phenylalaninate anion, shown in Fig. 3 of the main text. The $\Delta\Delta A$ signal is fit to the function

$$\Delta\Delta A = \alpha I^N / [1 + (I/I_{\text{sat}})^N], \tag{1}$$

where α is the amplitude, N is the photon order and I_{sat} is the saturation intensity. The best fit when $N = 3$ yields $\alpha = (9.80 \pm 0.46) \times 10^{-41}$ cm^6 W^{-3} and $I_{\text{sat}} = (1.15 \pm 0.02) \times 10^{13}$ W cm^{-2}. The value of N indicates that the photodetachment of phenylalaninate anion in aqueous environment occurs *via* a three-photon resonant enhancement process.

Section S2: Time-Dependent Density Functional Theory Calculations

We employ time-dependent density functional theory (TD-DFT), as implemented in the GAUSSIAN 16 program, to calculate the electronically excited states and the vertical excitation energies of the isolated phenylalaninate anion and microhydrated phenylalaninate anion $Phe(H_2O)_{10}^-$. Geometry optimization of the isolated and microhydrated phenylalaninate anion is performed by using B3LYP/6-311G++(d,p). The geometry is then used in the TD-DFT calculations of the excited states. For the isolated phenylalaninate anion, the calculations identify two excited states (labelled #13 and #14) that are located 5.8 eV above the ground state and whose one-photon transition from the ground state bears significant oscillator strength. Information on the molecular orbitals that comprise each electronically excited state, along with their configuration interaction expansion coefficients, are given below. Note that the orbitals labelled 43 and 44 are the HOMO-1 and HOMO of the phenylalaninate anion, shown in Fig. 8 of the main text.

```
Excited State 13:        Singlet-A   5.7869 eV   214.25 nm   f=0.0446
     43 → 47      0.13847
     43 → 48      0.19898
     43 → 49      0.17094
     43 → 50      0.13377
     43 → 53     -0.21341
     43 → 54     -0.19169
     44 → 49      0.13867
     44 → 50      0.35004
     44 → 51     -0.21800
     44 → 53      0.21867
     44 → 54      0.12298

Excited State 14:        Singlet-A   5.8302 eV   212.66 nm   f=0.0249
     43 → 47      0.28293
     43 → 48      0.40151
     43 → 50      0.14062
     43 → 53     -0.10366
     43 → 54     -0.10163
     44 → 49     -0.13654
     44 → 50     -0.14467
     44 → 51      0.24322
     44 → 53     -0.22775
     44 → 54     -0.13815
```

For the microhyrated phenylalaninate anion Phe$(H_2O)_{10}^-$, the calculations identified four excited states (labelled #8 to #11) that are located 5.8 eV above the ground state, where excited state #9 and #10 bear the largest oscillator strength. Note that the orbitals labelled 93 and 94 are the HOMO-1 and HOMO of the microhyrated phenylalaninate anion.

```
Excited State   8:         Singlet-A    5.7292 eV   216.41 nm   f=0.0038
     91 → 95     -0.10117
     93 → 95      0.66478
     93 → 100     0.10434

Excited State   9:         Singlet-A    5.8024 eV   213.68 nm   f=0.0199
     94 → 100     0.60595
     94 → 101     0.23865
     94 → 102    -0.11948
     94 → 103     0.12781

Excited State  10:         Singlet-A    5.8701 eV   211.21 nm   f=0.0252
     91 → 95     -0.12378
     92 → 95      0.11160
     92 → 96     -0.27994
     92 → 97     -0.16477
     92 → 98     -0.17985
     93 → 96      0.41906
     93 → 97     -0.15469
     93 → 98     -0.33356

Excited State  11:         Singlet-A    5.8905 eV   210.48 nm   f=0.0095
     91 → 95      0.66262
     93 → 96      0.10494
```
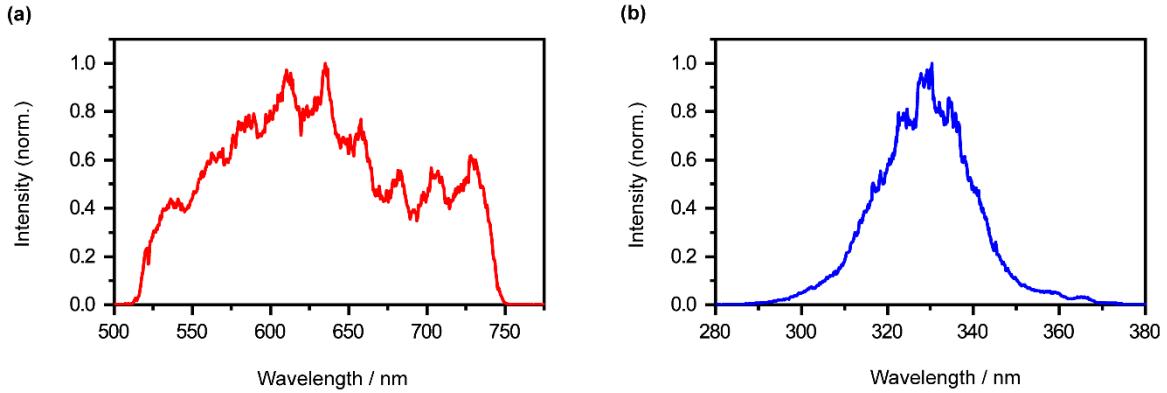
Fig. S1 (a) The visible-NIR ionizing pump spectrum ranges from 530 nm to 750 nm, with a center wavelength of 642 nm. **(b)** The broadband UV probe spectrum ranges from 290 nm to 360 nm.
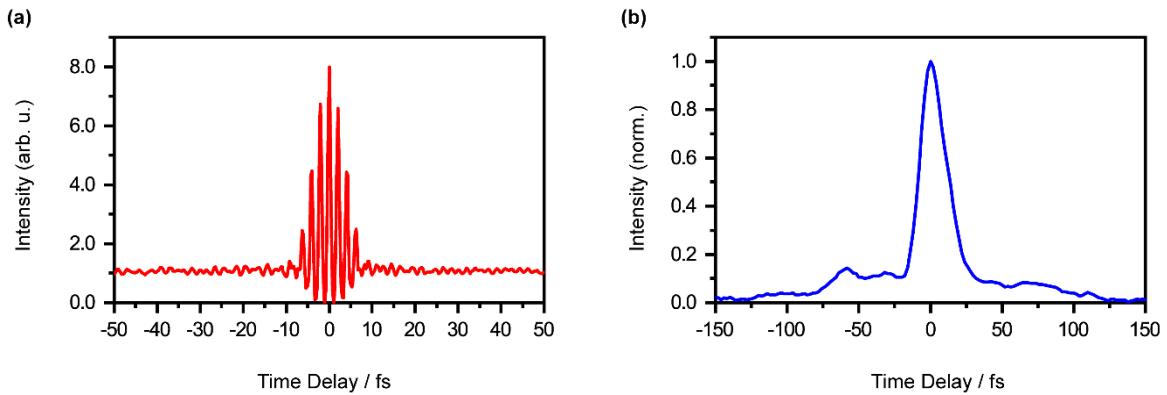

Fig. S2 (a) A second-order interferometric auto-correlation trace of the visible-NIR ionizing pump spectrum, measured in a 10-μm-thick, θ = 37.0 deg Type I BBO crystal, reveals a pulse duration with full-width half-maximum (FWHM) of 5.6 fs. **(b)** The visible-NIR pump – UV probe cross-correlation, measured *via* difference frequency mixing in a 10-μm-thick, θ = 37.0 deg Type I BBO crystal, reveals a FWHM of 24 fs.

5
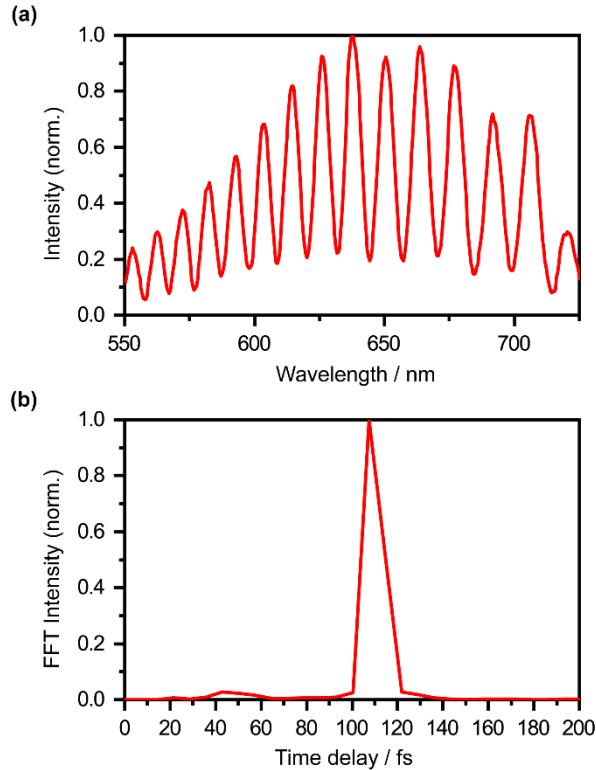
Fig. S3. (a) Spectrum of the pump beam reflected from the liquid water microjet target, revealing modulations due to spectral interferometry. **(b)** Normalized FFT spectrum of the spectral modulation, showing a time delay of ~107 fs between the front- and back reflections of the liquid microjet. Given the group index of 1.357 at 640-nm wavelength for liquid water, the thickness of the microjet is determined to be 12 μm. From the ~10-fs width of the peak, the uncertainty in the thickness of the liquid microjet is estimated to be ~1 μm.
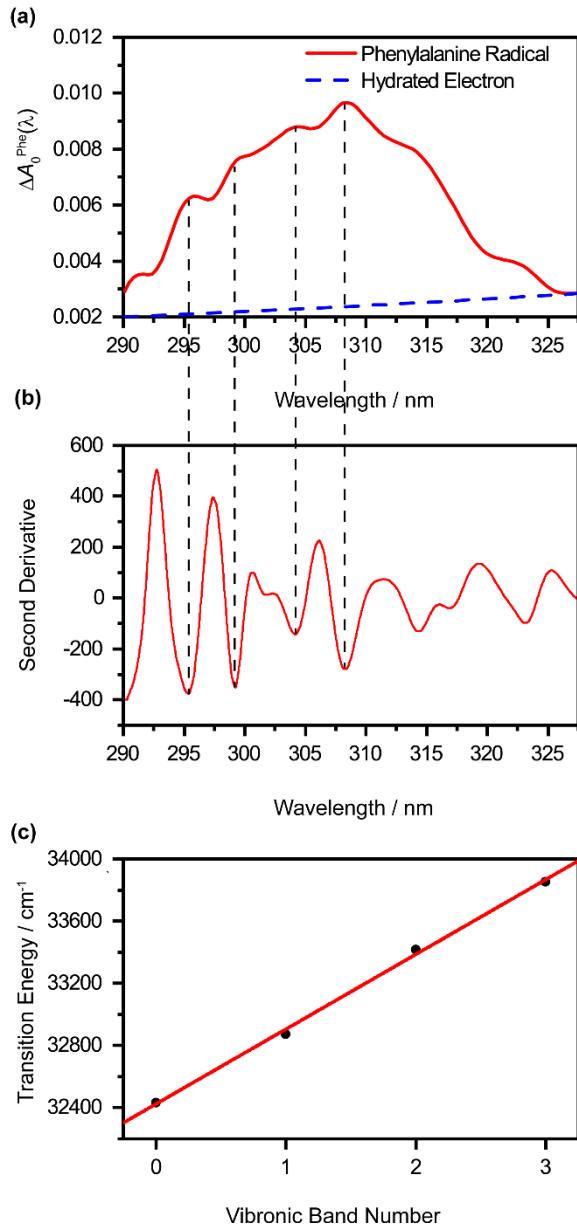
Fig. S4 (a) The wavelength-dependent offset values, $\Delta A_0(\lambda)$, obtained from the global fitting of photodetached aqueous phenylalaninate anion (in red) after taking the difference between the offset spectra of the aqueous phenylalaninate anion and aqueous sodium hydroxide. The residual vertical offset at long wavelength is most likely due to the absorption of the hydrated electron (in blue, dashed line). **(b)** Second-derivative spectrum of the molar extinction spectrum of the aqueous phenylalanine radical (Fig. 5b of the main text), showing the locations of the main peak and the vibronic bands. **(c)** A linear fit to the transition energies of the vibronic bands reveals a spacing of 482 ± 15 cm^{-1} for the vibronic progression.
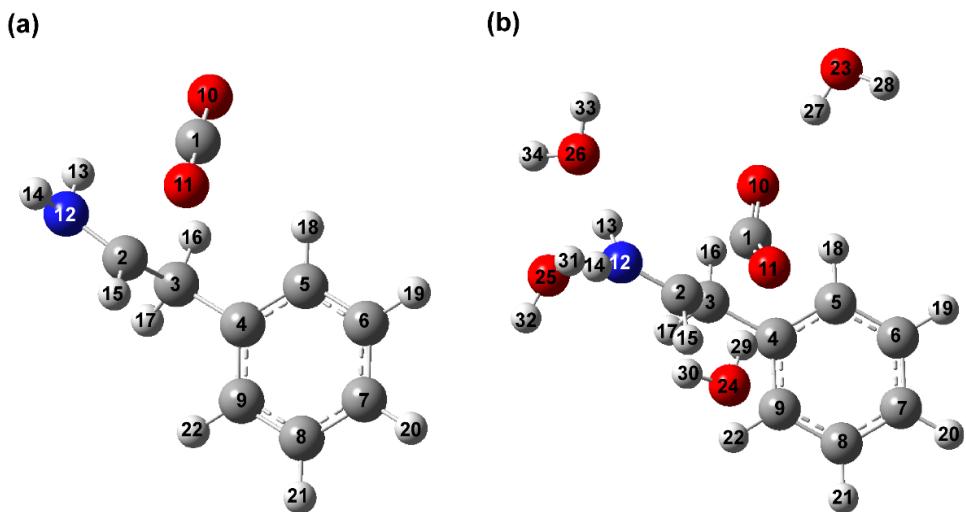
Fig. S5. The equilibrium geometry of **(a)** the phenylalanine radical and **(b)** the microhydrated phenylalanine radical, $Phe(H_2O)_4\bullet$. The microhydrated species includes the carboxyl ($-CO_2$) and amino ($-NH_2$) groups of the phenylalanine radical each hydrogen-bonded to two water molecules. The carbon, hydrogen, oxygen and nitrogen atoms are in gray, white, red and blue, respectively.
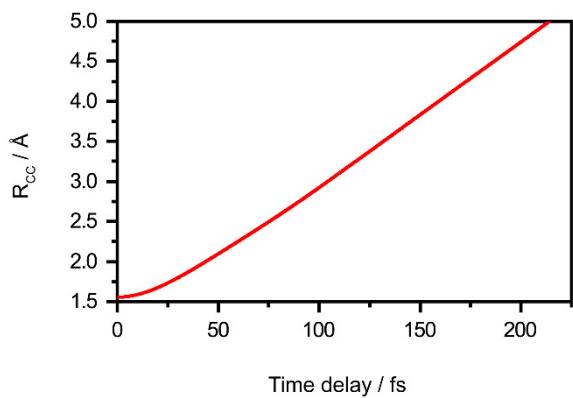
Fig. S6 Classical trajectory calculations performed using the potential energy curve calculated for the isolated Phe• radical reveal a duration of 214 fs for the C1–C2 bond to extend from the Franck-Condon region (1.557 Å) to 5.00 Å.

Table S1. Experimental FFT power, time-domain analysis results, and calculated frequencies of the phenylalanine radical in aqueous solution and their assignments. The calculated frequencies are based on the equilibrium geometry of the microhydrated phenylalanine radical, Phe(H_2O)$_{10}$•. The numbered assignments denote the benzene ring modes in the Wilson notation[1,2].

| FFT Freq (cm^{-1}) | Experimental | | | | Calc. Freq. (cm^{-1}) | Assignment |
| | Time-Domain Analysis | | | | | |
	Freq. (cm^{-1})	Amplitude (meV)	Dephasing Time (ps)	Phase (π-rad)		
486	479 ± 2	0.98 ± 0.15	0.64 ± 0.12	0.88 ± 0.05	515	16b
750	736 ± 6	3.98 ± 1.12	0.17 ± 0.03	1.00 ± 0.08	759	11
776	805 ± 6	0.52 ± 0.29	0.50 ± 0.28	1.18 ± 0.18	770	NH_2 wag
1003	1004 ± 1	4.23 ± 0.07	5.47 ± 0.73	1.76 ± 0.01	1015	12
1032	1031 ± 1	1.46 ± 0.08	2.83 ± 0.68	1.79 ± 0.02	1048	19a
1208	1208 ± 1	2.48 ± 0.13	0.98 ± 0.11	1.83 ± 0.02	1223	Chain CH_2 wag
1282	1269 ± 5	0.54 ± 0.18	0.71 ± 0.41	1.95 ± 0.15	1298	1 (19a, 12, 7a, 20a, 8a, 12, 6a)*
1319	1329 ± 5	0.36 ± 0.16	0.87 ± 0.71	0.28 ± 0.16	1351	Chain CH_2 wag / NH_2 twist
1601	1604 ± 2	0.30 ± 0.07	2.09 ± 1.41	0.69 ± 0.07	1640	9a / NH_2 wag
2005	1971 ± 22	1.61 ± 1.22	0.13 ± 0.07	0.58 ± 0.24	–	Overtone of 1003 cm^{-1}
1555	1555 ± 1	0.80 ± 0.05	7.37 ± 3.21	1.81 ± 0.01		Oxygen
2327	2329 ± 1	0.90 ± 0.06	15.38 ± 8.04	0.96 ± 0.01		Nitrogen

*Numbers in parentheses refers to minor contributions of phenyl vibrational modes to the main vibrational mode, in descending order of importance.

Table S2. Density functional theory (DFT)-calculated vibrational frequencies of the microhydrated 2-phenylethanamine and microhydrated phenylalanine radicals in an aqueous environment. The assignment of atoms and vibrational modes are based on the equilibrium geometries of the microhydrated phenylalanine radical, Phe$(H_2O)_4\bullet$, as shown in Fig. S5b. The numbered assignments denote the benzene ring modes in the Wilson notation.[1,2]

	Frequency / cm^{-1}		Assignment
	Microhydrated 2-phenylethanamine	**Microhydrated Phenylalanine Radical [Phe(H$_2$O)$_4$•]**	
1	59	67	CO_2 rock / 2-phenylethanamine rock
2	124	94	CO_2 twist
3	151	167	NH_2 twist / CH_2 twist / CH wag
4	220	344	CH_2 rock
5	286	319	16b
6	355	368	NH_2 twist / CH_2 rock
7	339	344	CH_2 Rock
8	415	415	16a
9	503	512	16b
10	604	610	Ring deformation
11	647	651	CO_2 bend / NH_2 twist
12	634	634	6b
13	757	755	NH_2 wag
14	711	712	11
15	762	761	11
16	833	837	6a
17	857	859	10a
18	924	902	17b
19	927	939	10b
20	993	975	NH_2 twist / 17b
21	987	993	17a
22	1006	1010	5
23	1015	1015	12

24	1046	1048	19a
25	1092	1105	19b
26	1151	1165	NH$_2$ rock / CH$_2$ twist
27	1173	1176	8b
28	1194	1199	14, 8b
29	1208	1234	NH$_2$ twist / CH$_2$ twist
30	1218	1221	CH$_2$ wag
31	1243	1299	1 (19a, 12, 7a, 20a, 8a, 12, 6a)*
32	1335	1332	15
33	1345	1354	CH$_2$ wag / NH$_2$ twist
34	1355	1367	3
35	1438	1458	CH$_2$ rock / CH rock
36	1474	1467	CH$_2$ symmetric bend
37	1478	1482	18b
38	1522	1525	18a
39	1616	1619	9b
40	1636	1640	9a / NH$_2$ wag
41	1669	1682	9a / NH$_2$ wag
42	2908	3017	CH$_2$ symmetric stretch
43	3002	3088	CH$_2$ asymmetric stretch
44	3139	3139	CH stretch
45	3154	3157	13
46	3156	3164	7b
47	3167	3172	20a (7a, 2, 13)*
48	3174	3180	20b
49	3186	3189	2
50	3453	3357	NH$_2$ symmetric stretch
51	3550	3468	NH$_2$ asymmetric stretch

*Numbers in parentheses refers to minor contributions of phenyl vibrational modes to the main

vibrational mode, in descending order of importance.

Table S3. Density functional theory (DFT)-calculated vibrational frequencies of the isolated phenylalanine radical and the microhydrated phenylalanine radical, with different microhydration configurations, all embedded in a polarizable continuum (PCM). The assignment of atoms and vibrational modes are based on the equilibrium geometries of the phenylalanine radical and the microhydrated phenylalanine radical, as shown in Fig. S5 and Fig. 9b of the main text. The numbered assignments denote the benzene ring modes in the Wilson notation.[1,2]

	Phe•	Phe(H$_2$O)$_3$•	Phe(H$_2$O)$_4$•	Phe(H$_2$O)$_{6a}$•	Phe(H$_2$O)$_{6b}$•	Phe(H$_2$O)$_9$•	Phe(H$_2$O)$_{10}$•	Assignment
				Calculated Vibrational Frequency (cm^{-1})				
1	8	7	23	15	22	22	18	CO$_2$ twist / Phenylalanine twist
2	15	44	24	53	42	47	63	CO$_2$ twist / Benzene twist
3	22	49	67	25	15	57	15	CO$_2$ rock / 2-phenylethanamine rock
4	31	24	32	36	31	32	28	Benzene twist
5	46	99	44	101	58	53	53	CO$_2$ rock / 2-phenylethanamine rock
6	62	54	94	287	107	81	49	CO$_2$ twist
7	100	105	173	175	166	103	178	Benzene rock
8	111	94	167	67	105	171	103	NH$_2$ twist / CH$_2$ twist / CH wag
9	281	158	319	315	314	299	323	16b
10	326	263	139	187	158	205	652	NH$_2$ rock
11	339	329	344	344	343	343	345	CH$_2$ rock

12	351	466	368	710	440	699	595	NH$_2$ twist / CH$_2$ rock
13	415	415	415	415	415	415	414	16a
14	505	505	512	513	511	515	515	16b
15	594	612	444	438	453	598	624	Ring deformation
16	617	296	610	610	575	598	611	Ring deformation
17	634	634	634	634	580	621	634	6b
18	637	636	651	647	658	658	691	CO$_2$ bend / NH$_2$ twist
19	658	653	668	674	670	684	682	CO$_2$ scissor
20	687	507	755	781	727	784	770	NH$_2$ wag
21	712	712	712	713	635	712	712	11
22	762	758	761	761	670	760	759	11
23	833	834	837	838	837	836	836	6a
24	857	858	859	859	859	858	858	10a
25	922	889	902	903	899	905	904	17b
26	929	931	939	940	936	940	940	10b
27	974	954	975	982	969	972	968	NH$_2$ twist / Chain CC stretch / 17b
28	988	992	993	992	992	992	992	17a
29	1005	1009	1010	1009	1009	1010	1010	5
30	1015	1015	1015	1015	1015	1015	1015	12
31	1047	1048	1048	1048	1048	1048	1048	19a

32	1113	1115	1100	1107	1105	1097	1092	19b
33	1155	1158	1156	1078	1165	1147	1147	NH$_2$ rock / CH$_2$ twist
34	1176	1177	1176	1177	1176	1176	1174	8b
35	1199	1200	1198	1199	1199	1200	1195	14, 8b
36	1231	1230	1230	1236	1234	1224	1203	NH$_2$ twist / CH$_2$ twist
37	1223	1221	1222	1221	1221	1221	1216	CH$_2$ wag
38	1298	1299	1298	1299	1299	1294	1230	1 (19a, 12, 7a, 20a, 8a, 12, 6a)*
39	1330	1330	1331	1332	1332	1330	1334	15
40	1351	1350	1352	1354	1354	1351	1343	CH$_2$ wag / NH$_2$ twist
41	1366	1365	1365	1367	1367	1365	1356	3
42	1276	1278	1261	1273	1267	1254	1371	CO$_2$ symmetric stretch
43	1448	1447	1458	1456	1458	1457	1432	CH$_2$ rock / CH rock
44	1468	1467	1466	1468	1467	1464	1473	CH$_2$ symmetric bend
45	1482	1482	1483	1482	1482	1483	1478	18b
46	1525	1525	1525	1525	1525	1525	1523	18a
47	1620	1620	1620	1619	1619	1620	1617	9b
48	1640	1640	1640	1640	1640	1640	1637	9a / NH$_2$ wag
49	1712	1715	1701	1698	1682	1650	1638	9a / NH$_2$ wag
50	1850	1847	1920	1884	1897	1960	2381	CO$_2$ asymmetric stretch
51	3026	3026	3013	3020	3017	3007	2920	CH$_2$ symmetric stretch

52	3000	3072	3088	3089	3080	3089	3090	CH$_2$ asymmetric stretch
53	3154	3160	3139	3134	3147	3136	3137	CH stretch
54	3155	3158	3157	3157	3157	3157	3157	13
55	3157	3164	3164	3164	3164	3164	3164	7b
56	3167	3172	3172	3172	3172	3172	3173	20a (7a, 2, 13)*
57	3175	3180	3180	3179	3179	3180	3180	20b
58	3187	3190	3189	3189	3190	3190	3190	2
59	3523	3556	3357	3280	3408	3260	3267	NH$_2$ symmetric stretch
60	3622	3668	3468	3380	3516	3404	3449	NH$_2$ symmetric stretch

*Numbers in parentheses refers to minor contributions of phenyl vibrational modes to the main vibrational mode, in descending order of importance

References

1.   E. B. Wilson, *Phys. Rev.*, 1934, **45**, 706-714.

2.   A. M. Gardner and T. G. Wright, *J. Chem. Phys.*, 2011, **135**, 114305.